Effect of interdot Coulomb repulsion on tunneling current through a double quantum dot system in the weak tunneling limit: Strong electron-phonon coupling

Igor G. Medvedev
A. N. Frumkin Institute of Physical Chemistry and Electrochemistry, Russian Academy of Sciences, Leninsky Prospect 31, 119991 Moscow, Russia

(Received 24 February 2009; revised manuscript received 9 June 2009; published 21 July 2009)

Pronounced effects of the interdot Coulomb repulsion on the tunnel current/gate voltage dependence at the ambient conditions are predicted for the double quantum dot system in the serial configuration immersed in the electrolyte solution in the case of the weak tunneling of electrons both between the dots and between the dots and leads. Electrons at the dots are coupled strongly to the classical phonon modes and Debye screening of the electric field is taken into account. The infinite intradot Coulomb repulsion limit is used. The effects consist of (i) a very large width of the maximum of the tunnel current/gate voltage dependence [of the order of $-k_BT\ln(k_0/k)$, where k_0 and k are the characteristic rates of the electron tunneling between the dots and between the dots and leads, respectively] in the limit $k_0/k\rightarrow 0$, (ii) the dependence of the positions of the maxima of the current/gate voltage curve and their widths on the sign of the difference of the electron energy levels δ of the quantum dots and the energy of the polaron shift, and (iii) narrow-width Coulomb blockade peaks in the tunnel current/gate voltage curve for $k_0 \geq k$. The dependence of the differential conductance on the gate voltage, the energy of the interdot Coulomb repulsion, the Debye screening length, and values of k_0/k and δ are studied. It is shown that the curves of the differential conductance/bias voltage dependence can be very different for different values of these parameters. These parameters also determine the position of the regions of the negative differential conductance which exist in the general case.

DOI: 10.1103/PhysRevB.80.035312 PACS number(s): 73.63.Kv, 73.23.Hk, 85.65.+h

I. INTRODUCTION

Recent advances in molecular electronics including the experimental realization of a molecular diode[1] are related with the successes in the investigation of the quantum dots. Particular attention was paid to the electron correlation effects which play an important role in the electron tunneling through quantum dot systems. These effects are rather well understood for arbitrary temperatures T (both for $T<T_K$ and $T>T_K$, where T_K is the Kondo temperature) both for the parallel and serial configurations in the case when the electron-phonon coupling is absent (see, e.g., Refs. 2–13, and references therein). In particular, for $T>T_K$, the intradot Coulomb repulsion U_{ii}, $i=1,2$, leads to the Coulomb blockade peaks in the differential conductance and in the tunnel current/gate voltage dependence. The account of the interdot Coulomb repulsion U_{12} in the case of the serial arrangement of the quantum dots destroys the symmetry between these peaks and can shift the position and change amplitudes of some peaks.[4,5,8]

Phonon-assisted tunneling in the double quantum dot system was considered only at low temperatures with neglect of the electron correlation effects (see, e.g., Ref. 14, and references therein) or at the room temperatures for the infinite intradot Coulomb repulsion and with neglect of the interdot one in the totally weak tunneling limit[15] (i.e., weak tunneling of electrons both between the dots and between the dots and leads). The effect of the intradot Coulomb repulsion on the tunnel current through a one-level quantum dot in the weak tunneling limit, in the case of the strong coupling of the electrons at the dot with the classical phonon modes, was considered in Ref. 16. One may suppose that, for $T>T_K$, the results of Refs. 2–13 together with those of Refs. 15 and 16 give a rather good insight into the effect of the finite intradot Coulomb repulsion on the tunnel current through the double quantum dots also in the case of the strong electron-phonon coupling. However, the interdot Coulomb repulsion U_{12} can be large enough in the case of the strongly localized electrons on the dots. Therefore, the effect of the interdot Coulomb repulsion on the tunnel current in the case of the strong electron-phonon interaction has to be studied. This problem can be investigated in detail within the totally weak tunneling limit when the rate equation method can be used.

In this paper we present the results of the study of the effect of the interdot Coulomb repulsion on the tunnel current through the double quantum dot system in the totally weak tunneling limit in the case of the strong electron-phonon coupling. In many cases U_{ii} is much larger than all other characteristic energies of the system so that the infinite intradot repulsion limit can be used. The double quantum dot system is immersed into the electrolyte solution. It permits to rule the tunnel current using two independent parameters: the bias voltage V as the source-drain voltage and the overvoltage η (the electrode potential vs a reference electrode inserted in the electrolyte solution) as the gate voltage. It also permits to study the effect of Debye screening of the electric field on the heights, positions, and widths of the peaks of the tunnel current/gate voltage dependence and on the differential conductance.

The structure of this paper is as follows. In Sec. II we describe the model and write the rate equations. A number of pronounced effects of the interdot Coulomb repulsion on the tunnel current/gate voltage dependence for different values of the other parameters of the system is predicted and studied in Sec. III. Section IV is devoted to the analysis of the differential conductance/bias voltage curves which are charac-

teristically different in the different regions of the parameter space. We summarize and conclude in Sec. V.

II. MODEL AND RATE EQUATIONS

The total system is described by the two-impurity Anderson Hamiltonian (where, however, the intradot Coulomb repulsion energies are very large) complemented by the term which takes into account the interdot Coulomb repulsion energy U_{12} between electrons having arbitrary spin projections. In addition, an electron at each dot interacts linearly with a classical phonon subsystem considered at room temperatures ($k_BT=0.025$ eV, where k_B is the Boltzmann constant). This phonon subsystem can represent slow vibrational modes of the solvent placed between the leads or classical intradot vibrational modes. Debye screening of the electrostatic potential in the electrolyte solution is also taken into account.

Let ε_{10} and ε_{20} be the energies of the spin-degenerate levels of the left and right dots, respectively, counted from the Fermi level of the left lead in the case when the electron-phonon coupling, interdot Coulomb interaction, and the external electric field are absent. Let ε_i be the same energies in the case when the interaction of electrons with the external electric fields is taken into account. Let t be the tunneling matrix element between the dots and, Δ_L and Δ_R, the widths of the electron levels of the first and second dots arising due to the tunneling of electrons between a lead and the nearest dot. The bias voltage V is defined in such a manner that eV equals the difference of the electrochemical potentials of the left and right leads. We consider below the totally weak tunneling limit when Δ_L, Δ_R, $|t|$, and $k_BT_K \ll k_BT \ll \lambda$ [or, more precisely,[17] $\Delta_L, \Delta_R \ll (k_BT\lambda)^{1/2}$] so that the rate equation method can be used.[2,3,18] Here λ is the polaron shift of each valence electron level due to the electron-phonon interaction. In the totally weak tunneling limit the tunneling is of sequential character with intermediate electron localization at the valence orbitals of the quantum dots after appropriate fluctuation of the phonon subsystem and its full relaxation so that the double quantum dot system can be characterized by a number of states (n_1,n_2) and their probabilities $P(n_1,n_2)$. Here n_i is the number of electrons at the ith dot ($n_i=0$ or 1 in the infinite intradot Coulomb repulsion limit). As in the case of the parallel configuration,[2,3] the probabilities $P(n_1,n_2)$ cannot be factorized as the products of the occupancy probabilities $P((n_1)$ and $P(n_2)$ for the corresponding single-electron levels. This is due to both the interdot Coulomb repulsion and the electron tunneling process. Only if $U_{12}=0$ and $t=0$ or $U_{12}=0$ and $V=0$, this factorization takes place. The effect of absence of the factorization even for $U_{12}=0$ in the case $V>0$, $t>0$ may be called the kinetic interdot correlation.

The probabilities $P(n_1,n_2)$ obey the kinetic equations

$$\frac{dP(0,0)}{dt} = -2k_{L1}(0,0)P(0,0) - 2k_{R2}(0,0)P(0,0) + k_{1L}(1,0)P(1,0) + k_{2R}(0,1)P(0,1), \quad (1)$$

$$\frac{dP(1,0)}{dt} = -k_{1L}(1,0)P(1,0) - k_{12}(1,0)P(1,0) - 2k_{R2}(1,0)P(1,0) + k_{21}(0,1)P(0,1) + 2k_{L1}(0,0)P(0,0) + k_{2R}(1,1)P(1,1), \quad (2)$$

$$\frac{dP(0,1)}{dt} = -k_{2R}(0,1)P(0,1) - k_{21}(0,1)P(0,1) - 2k_{L1}(0,1)P(0,1) + k_{12}(1,0)P(1,0) + 2k_{R2}(0,0)P(0,0) + k_{1L}(1,1)P(1,1), \quad (3)$$

and $P(1,1)=1-P(0,0)-P(1,0)-P(0,1)$. The rate constants $k_{\alpha\beta}(n_1,n_2)$, α, β=L, R, 1, and 2 describe the probabilities of electron transfer to (or from) the valence level of a given quantum dot from (or to) the corresponding lead [α=L,R; β=1,2 (or α=1,2; β=L,R)] or between the dots (α, β=1,2 or 2,1), where (n_1,n_2) denotes the state of the double quantum dot system prior electron transition. Factors 2 on the right-hand side (rhs) of Eqs. (1)–(3) are due to two possible spin projections of electrons in the leads. The subsequent discussion is limited to the symmetric contact, i.e., the leads are assumed to be made of the same metal and $z_2=L-z_1$, where L is the distance between the leads and z_i is the position of the ith quantum dot so that the polaron shift is the same for both valence levels.

As in Ref. 16, the rate constants $k_{\alpha\beta}(n_1,n_2)$ calculated up to the second order in the corresponding tunneling matrix element in the high-temperature limit for phonons have the form

$$k_{\alpha\beta}(n_1,n_2) = k\int \frac{d\varepsilon}{2k_BT} f_\alpha(\varepsilon)\exp\{-[\lambda - \Delta F_{\beta\alpha}(n_1,n_2) - \varepsilon + \varepsilon_F^\alpha]^2/4\lambda k_BT\}, \quad (4)$$

$$k_{\beta\alpha}(n_{1\beta},n_{2\beta}) = k_{\alpha\beta}(n_1,n_2)\exp[-\Delta F_{\beta\alpha}(n_1,n_2)/k_BT], \quad (5)$$

where α=L, β=1, $n_{11}=n_1+1$, $n_{21}=n_2$ or α=R, β=2, $n_{12}=n_1$, $n_{22}=n_2+1$. Here $f_\alpha(\varepsilon)$ are the Fermi functions of the left and right leads having the Fermi energies ε_F^α, the factor k is proportional to $\Delta_L(=\Delta_R)$ and the detailed balance principle was used in obtaining Eq. (5). $\Delta F_{1L}(0,0)=e(\xi\eta+\gamma_1 V) - k_BT\ln(2)$,[19] $\Delta F_{1L}(0,1)=\Delta F_{1L}(0,0)-U_{12}$, $\Delta F_{2R}(0,0) = e\xi\eta+e(\gamma_2-1)V+\varepsilon_{10}-\varepsilon_{20}-k_BT\ln(2)$, $\Delta F_{2R}(1,0) = \Delta F_{2R}(0,0)-U_{12}$, $\eta=\varphi_0-\varphi$ is the gate voltage, φ is the potential of the left lead, and φ_0 is the equilibrium potential of the left lead for the process of transfer of the electron, i.e., when $\varphi=\varphi_0$ and $V=0$, the process of the transfer of the electron to or from the first dot is in equilibrium at the left lead so that $2k_{L1}(0,0)=k_{1L}(1,0)$, ξ and γ_1, γ_2 quantify the effect of the gate voltage and bias voltage on the position of the electron energy levels of the dots (see Ref. 19) so that, for empty levels, $\varepsilon_1=\lambda-e\xi_1\eta-e\gamma_1V+k_BT\ln(2)$, $\varepsilon_2=\lambda-e\xi_2\eta - e\gamma_2V-\delta+k_BT\ln(2)$, where $\xi_1=\xi_2=\xi=1-\gamma_1-\gamma_2$ for the symmetric contact and $\delta=\varepsilon_{10}-\varepsilon_{20}$ is the asymmetry of the energy levels. Expressions for γ_1 and γ_2 are presented in Ref. 19. It should be noted that $\gamma_2 \geq \gamma_1$, $0<\gamma_i<1$, and γ_i depends on z_i/L and L_D/L, where L_D is the Debye length.

For example, $\gamma_i \approx 0$ and $\gamma_i \approx z_i/L$ for the cases of the full screening and weak screening, respectively.

$$k_{12}(1,0) = k_0 \exp\left\{-\frac{(\lambda_{12}-\Delta)^2}{4\lambda_{12}k_BT}\right\}, \tag{6}$$

$$k_{21}(0,1) = k_{12}(1,0)\exp\left\{-\frac{\Delta}{k_BT}\right\}. \tag{7}$$

Here the factor k_0 is proportional to $|t|^2$, $\lambda_{12}=2\lambda$ in the case when different phonon modes are coupled with electrons of the first and second quantum dots and $\Delta=\varepsilon_1-\varepsilon_2=\delta+(\gamma_2-\gamma_1)eV$. Since $\gamma_1 \neq \gamma_2$ in the general case, $\Delta \neq 0$ even if $\delta=0$.

It is worthwhile to discuss shortly the characteristic time scales of the classical phonon subsystem in connection with the problem of the polaron formation on the time scale $\tau_e=\hbar/\Delta_L$ of the electron tunneling events and the condition of the applicability of the weak tunneling limit [Eq. (4)] in the case under consideration. In addition to the usual time scale $\tau_{ph}=1/\omega_{av} \gg \tau_e$, where ω_{av} is the average frequency of the classical phonon modes, the second time scale τ_{cl} appears due to the electron-phonon coupling and the condition $k_BT/\hbar\omega_{av} \gg 1$. If one considers the phonon correlation function $U_{ph}(\tau)$ [see, e.g., p. 301 and Eq. (4.3.20) of Ref. 20] and expends the argument of the corresponding exponential function in series in $\hbar\omega_{av}\tau \ll 1$ and $(k_BT/\hbar\omega_{av})^{-1} \ll 1$, one obtains that the phonon correlation function is proportional to $\exp(-k_BT\lambda\tau^2/\hbar^2)$. Therefore, the classical phonon subsystem has an additional time scale $\tau_{cl}=\hbar/(k_BT\lambda)^{1/2}$ which characterizes the relaxation of this subsystem in the time interval between 0 and $\tau_{ph}=1/\omega_{av}$. Since $\tau_{cl} \ll \tau_e \ll \tau_{ph}$ [or $\Delta_L \ll (k_BT\lambda)^{1/2}$], the local polaron is formed on the time scale of the consequent tunneling events.

Another view on this problem is as follows. It can be shown that $k \sim \Delta_L/(k_BT\lambda)^{1/2}$. From the point of view of the Landau-Zener theory,[21] the parameter k is proportional to the Landau-Zener parameter, which, in its turn, is proportional to the ratio of $\tau_{nuclear}$ and τ_e where $\tau_{nuclear}=\tau_{cl}$ in the case under consideration. The weak tunneling limit implies that the Landau-Zener parameter is much smaller than 1 so that $\tau_{nuclear}=\tau_{cl} \ll \tau_e$. The same condition $\Delta_L \ll (k_BT\lambda)^{1/2}$ as the condition of the applicability of the weak tunneling limit was obtained in Ref. 17 as the condition opposite to that for the strong tunneling limit.

Calculations in the present paper are performed for values of k_0/k which lie within the range from 0.001 (the small k_0/k limit or $k_0/k \approx 0$) to 100 (the infinite k_0/k limit or $k_0/k \to \infty$). It can be shown that the ratio k_0/k is proportional to $|t|^2/(\Delta_L k_BT)$. The weak tunneling limit for the electron tunneling between dots takes place when $|t| \ll k_BT$ because one can neglect the effect of the splitting of the electron terms on the rate constant in this case. The smallest value of Δ_L, which is used in the literature (see, e.g., Ref. 4), has an order of 10^{-6} eV. Since Δ_L should be much smaller than $(\lambda k_BT)^{1/2}$ in the weak tunneling limit, one can consider $\Delta_L=0.01$ eV as an upper limit for Δ_L in the case when $\lambda=5k_BT$. Therefore, it is sufficient to take $\Delta_L=0.01$ eV and $|t|=0.0005$ eV$=0.02k_BT$ in order to obtain $k_0/k \sim 0.001$ (the small k_0/k limit). On the other hand, it is sufficient to take $\Delta_L=10^{-6}$ eV and $|t|=0.0016$ eV$=0.06k_BT$ in order to obtain $k_0/k \sim 100$ (the infinite k_0/k limit).

The steady-state tunnel current has the form

$$j = e[k_{12}(1,0)P(1,0) - k_{21}(0,1)P(0,1)], \tag{8}$$

where $P(1,0)$ and $P(0,1)$ are the steady-state solutions of rate Eqs. (1)–(3). These solutions are presented in the Appendix. Since $P(1,0)$ and $P(0,1)$ are lower than 1, it follows from Eqs. (6)–(8) that, with the exception of the case $L_D/L \to 0$, the tunnel current through the double quantum dot system tends to zero when $|V| \to \infty$. It leads to the appearance of two regions of the negative differential conductance which have a nature another than that considered in Ref. 7 and similar to that considered in Refs. 11 and 12.

III. ELECTRON CORRELATION EFFECTS IN THE CURRENT/GATE VOLTAGE DEPENDENCE

We address first the small k_0/k limit when the effect of the interdot Coulomb repulsion is most pronounced. We present the expressions for $P(1,0)$ and $P(0,1)$ in the limit $k_0/k \to 0$ for two opposite cases

$$P(1,0) = \frac{\exp[(eV-\Delta)/2k_BT]}{2\left\{\mathrm{ch}\left[\frac{eV-\Delta}{2k_BT}\right] + \mathrm{ch}\left[\frac{e\xi(V-2\eta)-\delta}{2k_BT}\right]\right\}} \tag{9}$$

for $U_{12}=0$ and

$$P(1,0) = \frac{\exp[(eV-\Delta)/2k_BT]}{2\mathrm{ch}\left\{\frac{eV-\Delta}{2k_BT}\right\} + \exp\left\{\frac{e\xi(V-2\eta)-\delta}{2k_BT}\right\}} \tag{10}$$

for $U_{12} \to \infty$. In both cases

$$P(0,1) = P(1,0)\exp\left\{-\frac{eV-\Delta}{k_BT}\right\}. \tag{11}$$

Equations (10) and (11) are obtained using Eqs. (5), (A7), (A8), and (A17).

It follows from Eqs. (8), (9), and (11) that, for $k_0/k \to 0$ and $U_{12}=0$, the probabilities $P(1,0)$, $P(0,1)$ and the tunnel current

$$j = \frac{ek_0 \exp(-\Delta^2/4\lambda_{12}k_BT)\exp(-\lambda_{12}/4k_BT)\mathrm{sh}(eV/2k_BT)}{2\mathrm{ch}\left\{\frac{[e\xi\eta + e\gamma_1 V]}{2k_BT}\right\}\mathrm{ch}\left\{\frac{[e\xi\eta + e(\gamma_2-1)V + \delta]}{2k_BT}\right\}} \tag{12}$$

tend to zero when $\eta \to \infty$. This is due to the fact that $P(1,1) \to 1$ in this limit so that the tunnel current cannot

flow. As a result, the dependences of $P(1,0)$, $P(0,1)$, and j on η have volcano-type shapes and take their maximum values at

$$\eta_{\max} = V/2 - \delta/2e\xi. \tag{13}$$

As is shown in the Appendix, Eq. (13) is valid for arbitrary values of k_0/k. The tunnel current given by Eq. (12) satisfies the identity $j(V,\eta,\delta)=-j(-V,-\eta,-\delta)$ for all values of λ. For arbitrary k_0/k, this identity takes place only in the large λ limit [see Eq. (A11)].

The width W at half maximum of the current/gate voltage curve for $k_0/k \to 0$ has the form

$$e\xi W = 2k_BT \ln\left\{2 + \mathrm{ch}\left(\frac{eV-\Delta}{2k_BT}\right) + \left[\left[2 + \mathrm{ch}\left(\frac{eV-\Delta}{2k_BT}\right)\right]^2 - 1\right]^{1/2}\right\} \tag{14}$$

and increases monotonously from $\approx 4k_BT\ln(1+2^{1/2})/e\xi$ for $|eV-\Delta| \ll 2k_BT$ to $\approx |eV-\Delta|/e\xi$ for $|eV-\Delta| \gg 2k_BT$. A value of $j(\eta_{\max})$ is proportional to $1/\mathrm{ch}^2[(eV-\Delta)/4k_BT]$ and decreases with the increase in Δ in the regions $\Delta > eV$ or $\Delta < eV$ even in the case when $\Delta \ll (4\lambda_{12}k_BT)^{1/2}$ so that the larger the distance between the levels ε_i, the smaller $j(\eta_{\max})$.

In contrast to the case when $U_{12}=0$, it follows from Eqs. (8), (10), and (11) that the probabilities $P(1,0)$, $P(0,1)$ and the normalized value of the tunnel current

$$j/ek_0 \exp(-\lambda_{12}/4k_BT) = \frac{2\exp(-\Delta^2/4\lambda_{12}k_BT)\mathrm{sh}(eV/2k_BT)}{2\mathrm{ch}\left\{\frac{eV-\Delta]}{2k_BT}\right\} + \exp\left\{\frac{e\xi(V-2\eta)-\delta]}{2k_BT}\right\}} \tag{15}$$

are finite in the limit $\eta \to \infty$ for $U_{12} \to \infty$ and $k_0/k \approx 0$. We have $P(1,1) \equiv 0$, $P(0,0) \to 0$, and $P(1,0)+P(0,1)=1$ in this case, that is, a manifestation of the strong Coulomb blockade. This results not only in the identity $P(1,1) \equiv 0$ but also in the abrupt increase in $P(1,0)$ with the increase in η at $V > 0$, $eV \gg k_BT$ (see curve 1 in Fig. 1) [for the sake of simplicity, we consider in this figure the fully symmetric case ($\varepsilon_{10}=\varepsilon_{20}$) and moderate Debye screening ($L_D/L=0.3$)]. The reason of such behavior is as follows. At $V>0$ and $\eta=0$ electron jumps to the dot 1 from the left lead. But it cannot jump easily to the dot 2 because $k_0/k \approx 0$. When η increases, $P(0,0)$ tends to zero so that $P(1,0)$ should increase because $P(0,1) \ll P(1,0)$ for $eV \gg k_BT$ [see Eq. (11) and curves 1 and 3 in Fig. 1]. If U_{12} is large but finite, $P(1,1)$ also starts to increase at rather large values of η which results in the decrease in $P(1,0)$ (see dashed line in Fig. 1). If U_{12} is still infinitely large but the ratio k_0/k increases, the electron can jump more easily from the dot 1 to the dot 2. As a result, $P(1,0)$ decreases with the increase in η after passing its maximum value while $P(0,1)$ begins to increase and becomes larger than $P(1,0)$ (see curves 2 and 4 in Fig. 1).

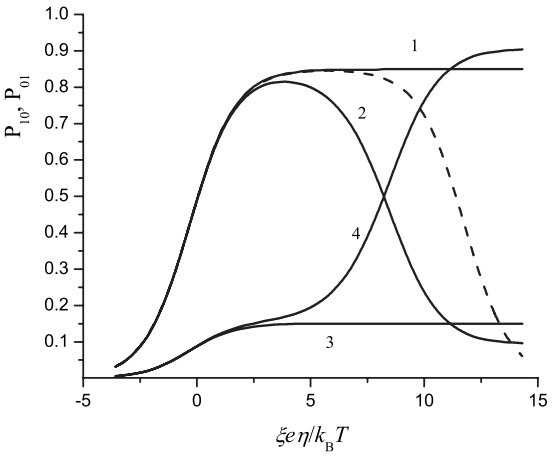

FIG. 1. The dependencies of the probabilities $P(1,0)$ and $P(0,1)$ on the gate voltage for $V=4k_BT$, $\lambda=5k_BT$, $\lambda_{12}=2\lambda$, $z_1/L=1-z_2/L=0.15$, $L_D/L=0.3$, $\delta=0$. Solid lines: $U_{12} \to \infty$. 1. $P(1,0)$ for $k_0/k=0$; 2. $P(1,0)$ for $k_0/k=0.01$; 3. $P(0,1)$ for $k_0/k=0$; and 4. $P(0,1)$ for $k_0/k=0.01$. The dashed line: $P(1,0)$ for $U_{12}=10k_BT$, $k_0/k=0$.

The dependence of $P(0,1)$ on η at $U_{12} \to \infty$ discussed above results in the gate voltage dependence of the normalized tunnel current. Using the large λ limit in the case when $k_0/k \approx 0$ it can be shown that the tunnel current takes its maximum value at $e\xi\eta_{\max,\infty} \approx -2k_BT\ln(k_0/k)/3$ and is almost independent of k_0/k for $\eta < \eta_{\max,\infty}$ [see Eqs. (A19)–(A21)]. Using Eqs. (4) and (8) in the opposite limit when $e\xi\eta \gg \lambda$ it can be shown that a width at half maximum W of the current/gate voltage curve equals approximately $-k_BT\ln(k_0/k)$ for $\delta=0$ [see Eq. (A34)]. These effects are demonstrated in Fig. 2 where the current/gate voltage dependences at $U_{12} \to \infty$ (solid lines) and $U_{12}=15k_BT$ (dashed line) for different values of k_0/k are presented. It follows from Fig. 2 that $j(\eta)$ curves have very large width W at small values of k_0/k (we note that $\xi \approx 0.36$ for $z_1/L=0.15$, L_D/L

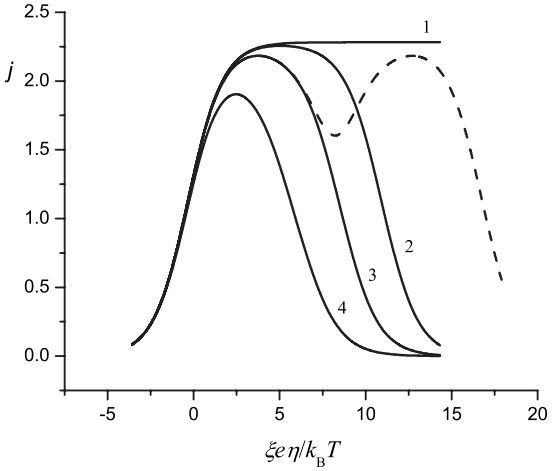

FIG. 2. Dependence of the tunnel current on the gate voltage. The current j is normalized to $ek_0\exp(-\lambda_{12}/4k_BT)$. The parameters are the same as in Fig. 1. Solid lines: $U_{12} \to \infty$. 1. $k_0/k \approx 0$; 2. $k_0/k=0.001$; 3. $k_0/k=0.01$; and 4. $k_0/k=0.1$. The dashed line: $U_{12}=15k_BT$, $k_0/k=0.01$.

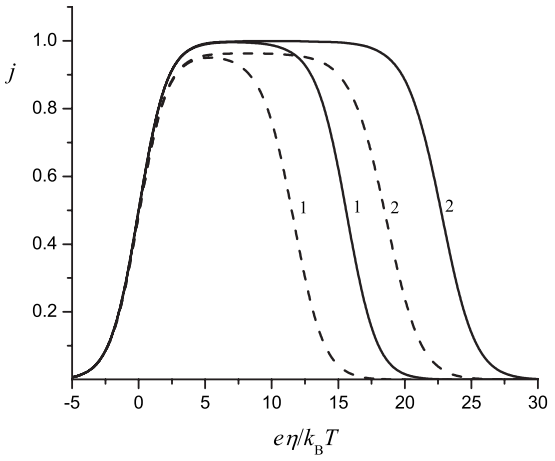

FIG. 3. Effect of λ and V on the tunnel current/gate voltage dependence for $k_0/k=0.01$, $\lambda_{12}=2\lambda$, $\delta=0$, $z_1/L=1-z_2/L=0.15$, $L_D/L=0.01$, and $U_{12}\to\infty$. Solid lines: $V=8k_BT$: 1. $\lambda=5k_BT$, 2. $\lambda=20k_BT$. Dashed lines: $V=4k_BT$: 1. $\lambda=5k_BT$, 2. $\lambda=20k_BT$. The current j is normalized to $ek_0\exp(-\lambda_{12}/4k_BT)$.

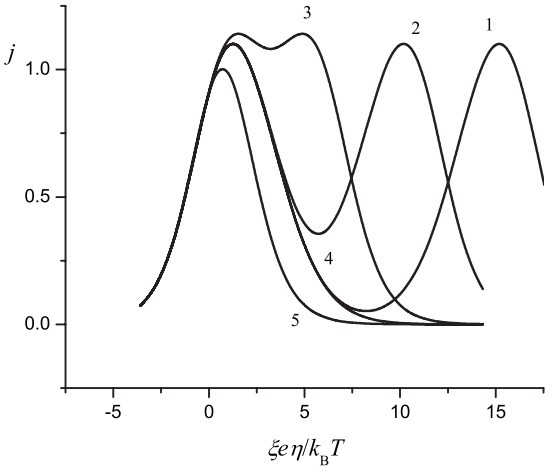

FIG. 4. Dependence of the tunnel current on the gate voltage for $k_0/k=1$. The current j is normalized to $ek_0\exp(-\lambda_{12}/4k_BT)$. The parameters are the same as in Fig. 1. 1. $U_{12}=15k_BT$; 2. $U_{12}=10k_BT$; 3. $U_{12}=5k_BT$; 4. $U_{12}\to\infty$; and 5. $U_{12}=0$.

=0.3). Figure 2 also shows that at finite U_{12} the $j(\eta)$ curve has the second (Coulomb blockade) peak. However, it overlaps strongly with the first peak for the values of U_{12} which generate this peak in the experimentally studied region of η ($\eta<1V$ or $e\xi\eta<14.3k_BT$). For $U_{12}<9k_BT$ both peaks of the $j(\eta)$ curve merge to one.

A consequence of the strong Coulomb blockade in the small k_0/k and large U_{12} limits is also the dependence of $\eta_{\max,\infty}$ and W on the energy λ of the polaron shift. This dependence has the same physical nature as the dependence of $\eta_{\max,\infty}$ and W on k_0/k since the ratio k_0/k enters actually all expressions through the parameter a given by Eq. (A12). The larger the λ, the smaller the rate constants $k_{12}(1,0)$ and $k_{21}(0,1)$. As a result, the energy $e\xi\eta_{\max,\infty}$ is shifted by $\lambda/6$ [see Eq. (A21)] and width increases as $\lambda/2$ [see Eqs. (A29) and (A34)]. Figure 3 demonstrates the dependence of $\eta_{\max,\infty}$ and W on λ for $\delta=0$ and two values of V. Figure 3 also shows that, for small $L_D=0.01$ ($\gamma_i\approx 0$ in this case), a value of $\eta_{\max,\infty}$ varies as $V/3$ but not as $V/2$ as for $U_{12}=0$.

When the ratio k_0/k increases and becomes larger than unity, the width W decreases and the position $\eta_{\max,\infty}$ of the maximum of the current/gate voltage dependences for $U_{12}\to\infty$ tends to a value which for $\delta=0$ coincides approximately with $\eta_{\max}$ for $U_{12}=0$ [see Fig. 4 and Eq. (A37)]. The position of the left maximum, $\eta_{\max,1}$, of the $j(\eta)$ curve for finite values of U_{12} also tends to the same value $\eta_{\max}$. When values of U_{12} and k_0/k are large enough, the first and second peaks of the current/gate voltage dependence becomes so narrow that the overlap between them is almost absent. In this case the behavior of the $j(\eta)$ curve near the second maximum is described approximately by the same equation as for $U_{12}\to\infty$ in which the energy $e\xi\eta$ is shifted by $-U_{12}$. As a result, the general shape of the $j(\eta)$ curves for finite U_{12} and $k_0\geq k$ is similar to that obtained for the one-level quantum dot[16] for finite values of the intradot Coulomb repulsion (see Fig. 1 of Ref. 16). Namely, the $j(\eta)$ curves for finite U_{12} in the region of the left maximum almost coincide with that for $U_{12}\to\infty$, the $j(\eta)$ curves demonstrate the second clear-cut Coulomb blockade peak which position tends to $\eta_{\max,2}=\eta_{\max}+U_{12}/\xi$ when $k_0/k\to\infty$ and $\delta=0$ [see Eq. (A41)], the height of the second peak is approximately the same as that of the first peak, the first and second peaks of the $j(\eta)$ curves merge at $U_{12}\leq U_{12*}$, where U_{12*} is the critical value which, in particular, equals $\approx 4k_BT$ for $k_0/k=1$. It should be noted that the critical values U_{12*} as well as the heights of peaks and their positions depend on the parameters V, λ, z_i/L, L_D/L, and δ. For the set of these parameters used for the calculation of the current/gate voltage dependences presented in Figs. 2 and 4 $U_{12*}\approx k_BT[4-\ln(k_0/k)]$ for $k_0/k\leq 1$. It should be also noted that, in totally weak tunneling limit, the bonding and antibonding states of the interacting quantum dots cannot appear so that the corresponding fine features in the current/gate voltage dependence obtained, e.g., in Refs. 4 and 8, are absent. The reason of the neglect of the effect of the mixing between the levels of the quantum dots on the current/gate voltage dependence is as follows. Since the difference between the bonding and antibonding levels has an order of $|t|$ (where $|t|\ll k_BT$ in the weak tunneling limit) and the smallest width of the current/gate voltage dependence has an order of k_BT, the fine features in the current/gate voltage dependence arising due to the mixing between the levels of the quantum dots are not observable in the case under consideration.

In contrast to Ref. 16, the peaks of the tunnel current/gate voltage dependence considered in the present paper have different physical nature than for the case of the one-level quantum dot. Unlike Ref. 16, the first and second peaks correspond to the transitions $L\to(0,0)$, $(1,0)\to(0,1)$, $(0,1)\to R$ and $(1,1)\to R$, $(1,0)\to(0,1)$, $L\to(0,1)$ (the hole current), respectively. The average positions of thermally fluctuating valence levels $E_1(n_1,n_2)$ and $E_2(n_1,n_2)$ of the first and second quantum dots (but not their fixed positions as in the absence of the electron-phonon coupling), counted from the Fermi levels of the left and right leads with due account of the interdot Coulomb repulsion, are given by the expressions $E_1(1,0)=-\Delta F_{1L}(0,0)=\varepsilon_1-\lambda$, $E_1(1,1)=-\Delta F_{1L}(0,1)$ and $E_2(0,1)=-\Delta F_{2R}(0,0)=\varepsilon_2+eV-\lambda$, $E_2(1,1)=-\Delta F_{2R}(1,0)$, respectively. At $\eta=\eta_{\max,1}$ or $\eta=\eta_{\max,2}$ the

corresponding energy levels $E_1(1,0)-k_BT\ln(2)$, $E_2(0,1)-k_BT\ln(2)$ or $E_1(1,1)-k_BT\ln(2)$, $E_2(1,1)-k_BT\ln(2)$ for all δ in the case when $U_{12}=0$ and for $\delta=0$ in the case when $U_{12}>U_{12*}$ lie close to the energy window (the energy gap between the Fermi levels of the left and right leads) on different sides from its center but at equal distances $|\Delta|/2$ from it. In particular case when $z_1=z_2$ and $\varepsilon_1=\varepsilon_2$ the positions of these levels coincide with the center of the energy window. As a result, the tunnel current reaches its maximum values when the corresponding energy levels lie symmetrically with respect to the center of the energy window.

When $|\delta|\gg|eV|$, k_BT and $U_{12}>U_{12*}$, the electron correlation effects manifests itself through the additional dependence of the positions $\eta_{\max,1}$ and $\eta_{\max,2}$ of the first and the second peaks of the current/gate voltage dependence and their widths on the parameters V, L_D, and δ as compared with the case $\delta=0$ when $\eta_{\max,1}\approx\eta_{\max,\infty}\approx\eta_{\max}$, $\eta_{\max,2}\approx\eta_{\max}+U_{12}$. In particular, a value of $\eta_{\max,\infty}\approx\eta_{\max,1}$ depends on the sign of δ for all values of k_0/k. As follows from Eqs. (A25)–(A27) and (A39), $e\xi\eta_{\max,\infty}$ varies as $-\delta$ for $\delta>0$ and is independent of δ for $\delta<0$. The width also depends on δ for small k_0/k or $k_0\sim k$ [see Eqs. (A30) and (A34)] and is larger for $\delta<0$ but, in contrast to the case when $U_{12}=0$, is independent of V, λ, z_i/L, L_D/L, and δ for $k_0/k\gg1$ (see the Appendix). Figure 5 demonstrates the effect of $|\delta|$ and the sign of δ on the curves of the current/gate voltage dependence. Figure 5 shows that the positions of the maxima of $j(\eta)$ curves are independent of δ for $\delta<0$ The difference of values of $e\xi\eta_{\max,\infty}$ for curves presented in Fig. 5(a) is well described by Eqs. (A26) and (A27). The widths of the maxima are larger for $\delta<0$ in the small k_0/k limit [Fig. 5(a)] and are independent of δ for $k_0/k\gg1$ [Fig. 5(b)].

The dependence of $\eta_{\max,2}$ on δ is opposite to that for $\eta_{\max,1}$. For large k_0/k, a value of $\eta_{\max,2}$ is independent of δ for $\delta>0$ and varies as $|\delta|$ for $\delta<0$ [Eq. (A42)]. Figure 6(a) shows that, for $\delta>0$, the position of the Coulomb blockade peak almost coincides with that for $\delta=0$. However, the position of the left peak is shifted to the left by $\approx\delta$. On the contrary, for $\delta<0$, the position of the left peak almost coincides with that for $\delta=0$ but the position of the Coulomb blockade peak is shifted to the right by $\approx|\delta|$ relative to $\eta_{\max,2}$ for $\delta=0$.

In contrast to the case when $U_{12}=0$ or $U_{12}>U_{12*}$, $\delta=0$, the positions of the energy levels $E_1(1,0)-k_BT\ln(2)$, $E_2(0,1)-k_BT\ln(2)$ and $E_1(1,1)-k_BT\ln(2)$, $E_2(1,1)-k_BT\ln(2)$ are asymmetric with respect to the center of the energy window for $|\delta|\gg|eV|$, k_BT, $U_{12}>U_{12*}$, large k_0/k and $\eta=\eta_{\max,1}$, $\eta_{\max,2}$. At $\eta=\eta_{\max,1}$, the lower energy level lies at one of the Fermi levels of the leads [e.g., $E_1(1,0)-k_BT\ln(2)$ lies at the Fermi level of the left lead for $\delta<0$ and $E_2(0,1)-k_BT\ln(2)$ lies at the Fermi level of the right lead for $\delta>0$] whereas the higher energy level is shifted upward by $|\Delta|$. On the contrary, at $\eta=\eta_{\max,2}$, the higher energy level lies at one of the Fermi levels of the leads [e.g., $E_1(1,0)-k_BT\ln(2)$ lies at the Fermi level of the left lead for $\delta>0$ and $E_2(0,1)-k_BT\ln(2)$ lies at the Fermi level of the right lead for $\delta<0$] whereas the lower energy level is shifted downward by $|\Delta|$.

It can be shown that the heights $j(\eta_{\max,1})$ and $j(\eta_{\max,2})$ of the peaks are independent of the sign of δ for $|eV|\ll k_BT$ and decrease with the increase in $|\delta|$. When $|\delta|$ and $|eV|$ have the same order, the strong dependence of the heights of the peaks on the sign of δ appears for $|\Delta|\ll(4\lambda_{12}k_BT)^{1/2}$. As follows from Eq. (A23), $j(\eta_{\max,1})$ depends on $eV-\Delta$ for $k_0/k\ll1$ and, therefore, is larger for $\delta>0$ at given $|\delta|$ and $V>0$ [see curves 1 in Fig. 5(a)]. Then $|\Delta|\sim(4\lambda_{12}k_BT)^{1/2}$, the first exponential factor on the rhs of Eq. (A23) plays an important role so that for $|\delta|=7k_BT$ the heights of the peaks are almost independent of the sign of δ [see curves 2 in Fig. 5(a)].

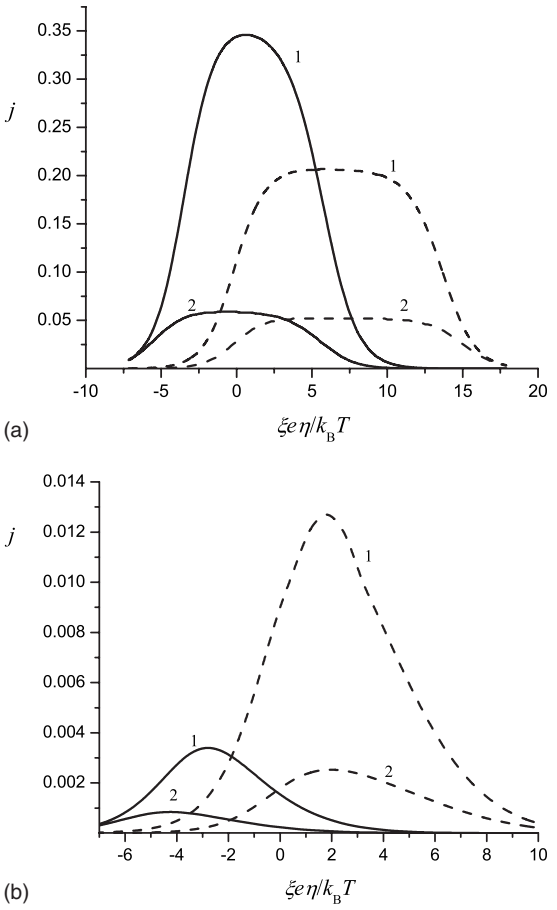

FIG. 5. Effect of δ on the tunnel current/gate voltage dependence for $V=4k_BT$, $\lambda=5k_BT$, $\lambda_{12}=2\lambda$, $z_1/L=1-z_2/L=0.15$, $L_D/L=0.3$, and $U_{12}\to\infty$. 1. $|\delta|=5k_BT$; 2. $|\delta|=7k_BT$. Solid lines: $\delta>0$. Dashed lines: $\delta<0$. (a) $k_0/k=0.01$, (b) $k_0/k=100$. The current j is normalized to $ek_0\exp(-\lambda_{12}/4k_BT)$.

On the contrary, for $k_0/k\gg1$, values of $j(\eta_{\max,1})$ and $j(\eta_{\max,2})$ depend mainly on $|\Delta|$ [see Eq. (A38)] and are larger for $\delta<0$ because $(\gamma_2-\gamma_1)eV>0$ for $V>0$ that leads to the smaller values of $|\Delta|$ [see Figs. 5(b) and 6(a)]. However, for intermediate values of $k_0/k\sim1$, all the peaks of the tunnel current shown in Fig. 6(b) have approximately the same heights which are almost independent of the sign of δ for $L_D/L=0.3$. It should be noted that the heights of the peaks of $j(\eta)$ depend also on L_D/L at given δ due to the strong dependence of Δ on $\gamma_2-\gamma_1$. Figure 6(c) shows the effect of Debye screening on the heights of the peaks of $j(\eta)$. The increase in the screening ($L_D/L=0.1$, $\gamma_2-\gamma_1$ is small) leads to the significant dependence of the heights of the peaks on the sign of δ since $|\Delta|$ for $\delta<0$ becomes larger whereas Δ

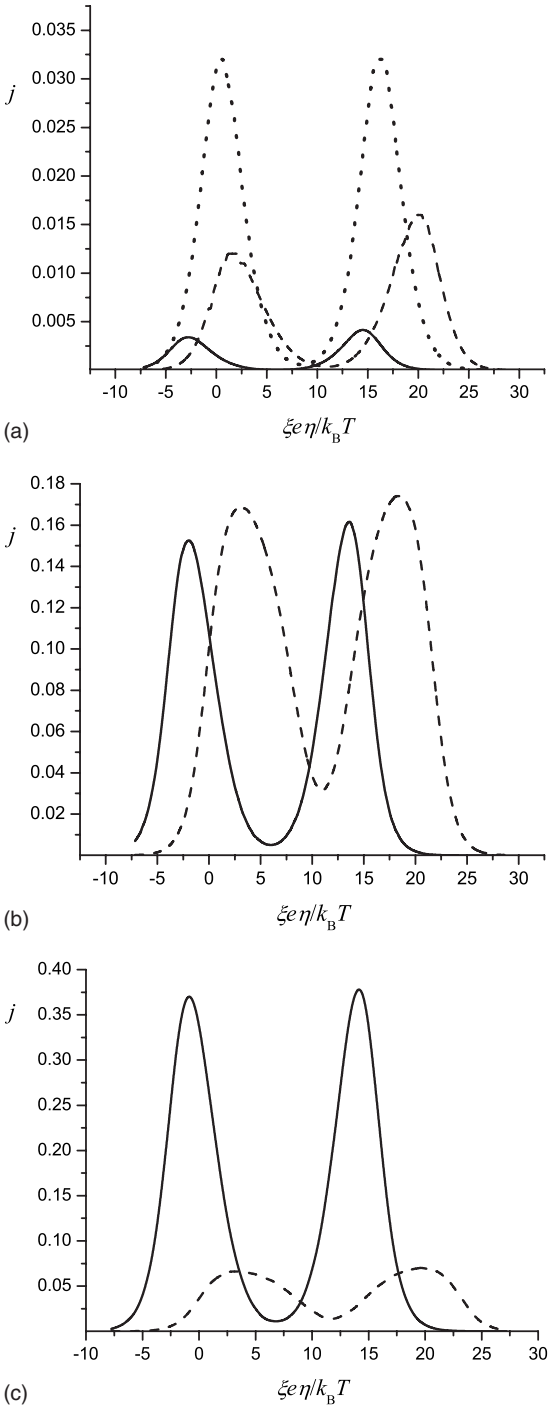

FIG. 6. Effect of δ, k_0/k, and L_D/L on the heights, widths, and positions of peaks of the tunnel current/gate voltage dependence for $V=4k_BT$, $\lambda=5k_BT$, $\lambda_{12}=2\lambda$, $z_1/L=1-z_2/L=0.15$, and $U_{12}=15k_BT$. Solid lines: $\delta=5k_BT$. Dashed lines: $\delta=-5k_BT$. (a) $k_0/k=100$, $L_D/L=0.3$. Dotted line: $\delta=0$. (b) $k_0/k=1$, $L_D/L=0.3$. (c) $k_0/k=100$, $L_D/L=0.1$. The current j is normalized to $ek_0\exp(-\lambda_{12}/4k_BT)$.

for $\delta>0$ becomes smaller as compared with the case when $L_D/L=0.3$. Figures 6(b) and 6(c) also show that, as for small values of k_0/k, the widths of the peaks of $j(\eta)$ curves for $k_0/k=1$ still depend on the sign of δ and are larger for negative δ.

IV. DIFFERENTIAL CONDUCTANCE

Since $k_{12}(1,0)$ and $k_{21}(0,1)$ depend exponentially on $(\lambda_{12}-\Delta)^2/(4\lambda_{12}k_BT)^{1/2}$, one can suggest that, for small values of k_0/k or for $k_0\sim k$, the tunnel current as a function of a bias voltage is large when

$$eV_{*\pm}=(\pm\lambda_{12}-\delta)/(\gamma_2-\gamma_1), \tag{16}$$

where the difference $\gamma_2-\gamma_1=\mathrm{sh}[(z_2-z_1)/2L_D]/\mathrm{sh}(L/2L_D)$ is smaller than 1 for $z_2-z_1<L$ and increases monotonously from ≈ 0 for $L_D/L\ll 1$ to $(z_2-z_1)/L$ for $L_D/L\gg 1$ (e.g., $\gamma_2-\gamma_1=0.57$ for $z_1/L=0.15$ and $L_D/L=0.3$). In all cases $|eV_{*\pm}|\sim\lambda_{12}/(\gamma_2-\gamma_1)\gg\lambda$ for $V_{*+}>0$, $\delta\leq 0$ or $V_{*-}<0$, $\delta\geq 0$. It can be shown that, for $|eV|\gg\lambda$, $|e\xi\eta|$, $|\delta|$, and all values of U_{12} and k_0/k, the probabilities $P(1,0)$ and $P(0,1)$ tend to 1 for $V>0$ and $V<0$, respectively [see, e.g., Eqs. (9)–(11) obtained for the case when $k_0/k\ll 1$]. This fact is obvious since, for, e.g., $V>0$ and the parameters under consideration, the energy level ε_1 lies deeply under the Fermi level of the left lead whereas the energy level ε_2 lies much higher with respect to the Fermi level of the right lead. Therefore, as follows from Eq. (8), the tunnel current in the neighborhoods of the points $V_{*\pm}$ equals approximately $ek_{12}(1,0)$ or $-ek_{21}(0,1)$.

In fact, values of $|eV_{*\pm}|$ are not very large so that $P(1,0)$ or $P(0,1)$ is smaller than 1. However, these probabilities vary slowly with V in the neighborhoods of the points $V_{*\pm}$ as compared with the exponential factors. Therefore, the positions of the maxima of the current/bias voltage dependence indeed coincide approximately with the points $V_{*\pm}$. When $|V|>|V_{*\pm}|$ and $L_D/L>0$, the tunnel current decreases and tends to zero that leads to the existence of two regions of the negative differential conductance.

The physical meaning of this result is as follows. When $V>0$, a value of the tunnel current is governed by the electron transitions from the first quantum dot to the second one. The energy of the occupied electron level of the first quantum dot and the energy of the empty one of the second dot equal $-2\lambda+\varepsilon_1$ and ε_2, respectively. The condition of the coincidence of these levels is $V=V_{*+}$. Analogously, at $V<0$, the condition of the coincidence of the empty energy level of the first quantum dot and the occupied energy level of the second one is $V=V_{*-}$. When $|V|>|V_{*\pm}|$, the energy gap between levels increases that leads to the decrease in the tunnel current. Therefore, as in Refs. 11 and 12, the regions of the negative differential conductance appear due to the increasing noncoincidence of the energy levels of quantum dots. However, in contrast to Refs. 11 and 12, in the totally weak tunneling limit with account of the strong electron-phonon interaction and the Debye screening effect, the condition of the coincidence of the energy levels is determined by the energy of the polaron shift and a value of the Debye screening length. As a result, the widths of the peaks of the differential conductance/bias voltage curves depend not on the widths Δ_L and Δ_R of the electron levels of the quantum dots but are proportional to $(\lambda k_BT)^{1/2}/(\gamma_2-\gamma_1)$.

Using Eq. (8) for the tunnel current and assuming a slow variation in the probabilities $P(1,0)$ and $P(0,1)$ with V in the neighborhood of the points $V_{*\pm}$, it can be shown that the

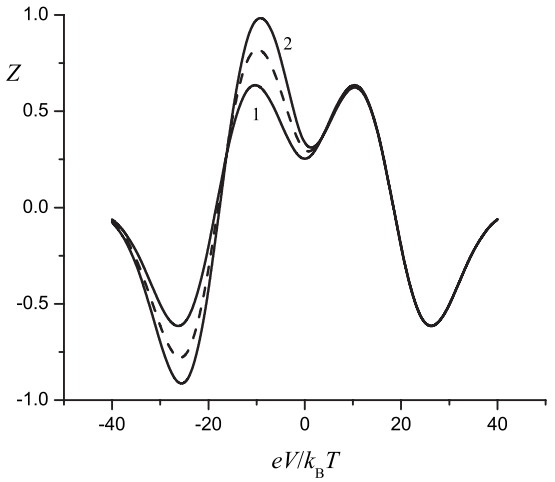

FIG. 7. Effect of U_{12} on the dependence of the differential conductance on the bias voltage for $\eta=\delta=0$, $\lambda=5k_BT$, $\lambda_{12}=2\lambda$, $z_1/L=1-z_2/L=0.15$, $L_D/L=0.3$, and $k_0/k=0.01$. Solid lines: 1. $U_{12}=0$; 2. $U_{12}\to\infty$. The dashed line: $U_{12}=1k_BT$. Differential conductance is normalized to $ek_0\exp(-\lambda_{12}/4k_BT)/k_BT$.

differential conductance $Z(V,\eta,\delta)=dj/d(eV)$ takes its maximum and minimum values at the points

$$V_{\max,+}\approx V_{*+}-2(\lambda k_BT)^{1/2}/(\gamma_2-\gamma_1),$$

$$V_{\max,-}\approx V_{*-}+2(\lambda k_BT)^{1/2}/(\gamma_2-\gamma_1) \quad (17)$$

and

$$V_{\min,+}\approx V_{*+}+2(\lambda k_BT)^{1/2}/(\gamma_2-\gamma_1),$$

$$V_{\min,-}\approx V_{*-}-2(\lambda k_BT)^{1/2}/(\gamma_2-\gamma_1), \quad (18)$$

respectively. It can also be shown that $Z(V_{\max,\pm})=-Z(V_{\min,\pm})\approx k_0(\gamma_2-\gamma_1)e^{-1/2}/[2(\lambda k_BT)^{1/2}]$. The width at half maximum of the peaks of the $Z(V)$ curve equals approximately $2(\lambda k_BT)^{1/2}/(\gamma_2-\gamma_1)$. It is also obvious that the zeros of $Z(V)$ equal approximately $V_{*\pm}$.

Figures 7–9 demonstrate the effect of U_{12}, η, and δ on the differential conductance/bias voltage dependence for $k_0/k=0.01$. Figures 7 and 8 show that, in accordance with Eqs. (17) and (18), the positions of the points of maxima and minima of $Z(V)$ curves are independent of U_{12} and η. On the other hand, Fig. 9 shows that these positions depend on δ and, in the region $V>0$ for $\delta\leq 0$ and in the region $V<0$ for $\delta\geq 0$, are well described by Eqs. (17) and (18). It follows from the identity $j(V,\eta,\delta)=-j(-V,-\eta,-\delta)$ for the tunnel current which is valid for $U_{12}=0$ for small values of k_0/k and arbitrary λ or for arbitrary k_0/k in the large λ limit that, under the same conditions, $Z(V,\eta,\delta)=Z(-V,-\eta,-\delta)$. As can be seen from Figs. 7–9 this identity indeed satisfies for $U_{12}=0$. In particular, $Z(V)$ is an even function of V for $U_{12}=\eta=\delta=0$.

However, for $U_{12}>0$, this identity as well as the identity $j(V,\eta,\delta)=-j(-V,-\eta,-\delta)$ for the tunnel current are not valid. This manifestation of the electron correlation effects follows formally from Eqs. (9)–(11). These equations show that, for $U_{12}=0$, a value of $P(1,0)$ at given V, η, and δ equals $P(0,1)$ at $-V$, $-\eta$, and $-\delta$, respectively. These equations also show that, for rather large positive values of V, the probabilities $P(1,0)$ are approximately the same both for $U_{12}=0$ and $U_{12}>0$ so that the probabilities $P(1,0)$ at $V=V_{*+}$ are almost the same both for $U_{12}=0$ and for $U_{12}\to\infty$ (see Fig. 7). However, although $P(1,0)$ at $V=V_{*+}$ equals $P(0,1)$ at $V=V_{*-}$ for $U_{12}=0$ and $\eta=\delta=0$, it is not the case for $U_{12}>0$. In contrast, we have that $P(0,1)$ at $V=V_{*-}$ is larger than $P(1,0)$ at $V=V_{*+}$ for $U_{12}>0$ (see Fig. 7). This difference between $P(1,0)$ and $P(0,1)$ depends on L_D/L and decreases for large values of L_D/L [see Fig. 10(a)]. The physical meaning of such behavior of $P(1,0)$ and $P(0,1)$ is as follows. For $U_{12}=0$, the equality between $P(1,0)$ at $V=V_{*+}$ and $P(0,1)$ at $V=V_{*-}$ for $\eta=\delta=0$ is ruled by the symmetry between the electron and hole currents. When $U_{12}>0$, the asymmetry in the positions of the electron energy levels of the quantum dots at different signs of the bias voltage should be taken into account. When $V>0$ and $\eta=\delta=0$, the level $E_1(1,0)-k_BT\ln(2)$ is situated at $-\gamma_1eV$ below the Fermi level of the left lead. In contrast, for $V<0$ and $\eta=\delta=0$, the level $E_2(0,1)-k_BT\ln(2)$ lies at $e(1-\gamma_2)|V|$ below the Fermi level of the right lead. Since $1-\gamma_2>\gamma_1$, the sym-

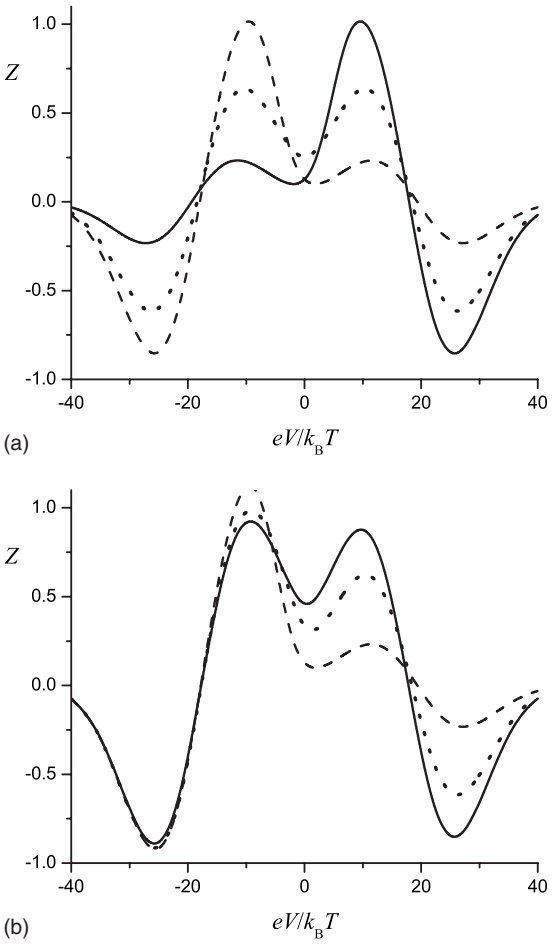

FIG. 8. Effect of η on the dependence of the differential conductance on the bias voltage for $\delta=0$, $\lambda=5k_BT$, $\lambda_{12}=2\lambda$, $z_1/L=1-z_2/L=0.15$, $L_D/L=0.3$, $k_0/k=0.01$. (a) $U_{12}=0$; (b) $U_{12}\to\infty$. Solid line: $\eta=5k_BT$, dashed line: $\eta=-5k_BT$, and dotted line: $\eta=0$. Differential conductance is normalized to $ek_0\exp(-\lambda_{12}/4k_BT)/k_BT$.

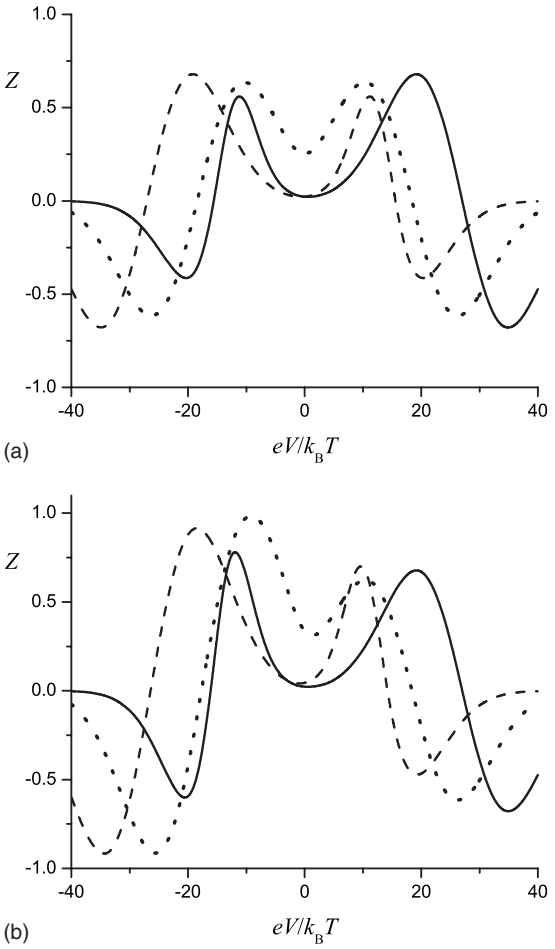

FIG. 9. Effect of δ on the dependence of the differential conductance on the bias voltage for $\eta=0$, $\lambda=5k_BT$, $\lambda_{12}=2\lambda$, $z_1/L=1-z_2/L=0.15$, $L_D/L=0.3$, and $k_0/k=0.01$. (a) $U_{12}=0$; (b) $U_{12}\to\infty$. Solid line: $\delta=-5k_BT$, dashed line: $\delta=5k_BT$, dotted line: $\delta=0$. Differential conductance is normalized to $ek_0\exp(-\lambda_{12}/4k_BT)/k_BT$.

metry between the positions of the levels in the cases when $V>0$ and $V<0$ is broken so that $P(0,1)$ at $V<0$ is large than $P(1,0)$ at $V>0$. This symmetry takes place only when the ratio L_D/L is large, since then $1-\gamma_2=\gamma_1=z_1/L$.

As for the differential conductance at the zero bias voltage, $Z(0)$, it is shown in the Appendix [see Eq. (A14)] that for $U_{12}=0$, $Z(0)$ is independent of L_D/L at $\eta=0$, depends only on the absolute value of δ in this case and decreases when it increases [see Fig. 9(a)]. Analogously, $Z(0)$ depends on the absolute value of η at $\delta=0$ and decreases when it increases [see Fig. 8(a)]. In contrast, as can be readily shown from Eq. (15), the differential conductance $Z(0)$ for $U_{12}\to\infty$ depends on the signs of η and δ and is larger for $\eta>0$ and $\delta>0$ [see Fig. 8(b)]. It can also be shown that, for arbitrary L_D/L and $\eta=\delta=0$, $Z(0)$ for $U_{12}\to\infty$ equals 4/3 of $Z(0)$ for $U_{12}=0$ at small k_0/k [see Figs. 7 and 10(b)] and $Z(0)$ for $U_{12}\to\infty$ equals 2/3 of $Z(0)$ for $U_{12}=0$ at large k_0/k [see Fig. 11(b)].

We have already discussed above the effect of the small Debye screening (large values of L_D/L) on the relation between $P(1,0)$ at $V=V_{*+}$ and $P(0,1)$ at $V=V_{*-}$. In the opposite case of small values of L_D/L the strong Debye screening

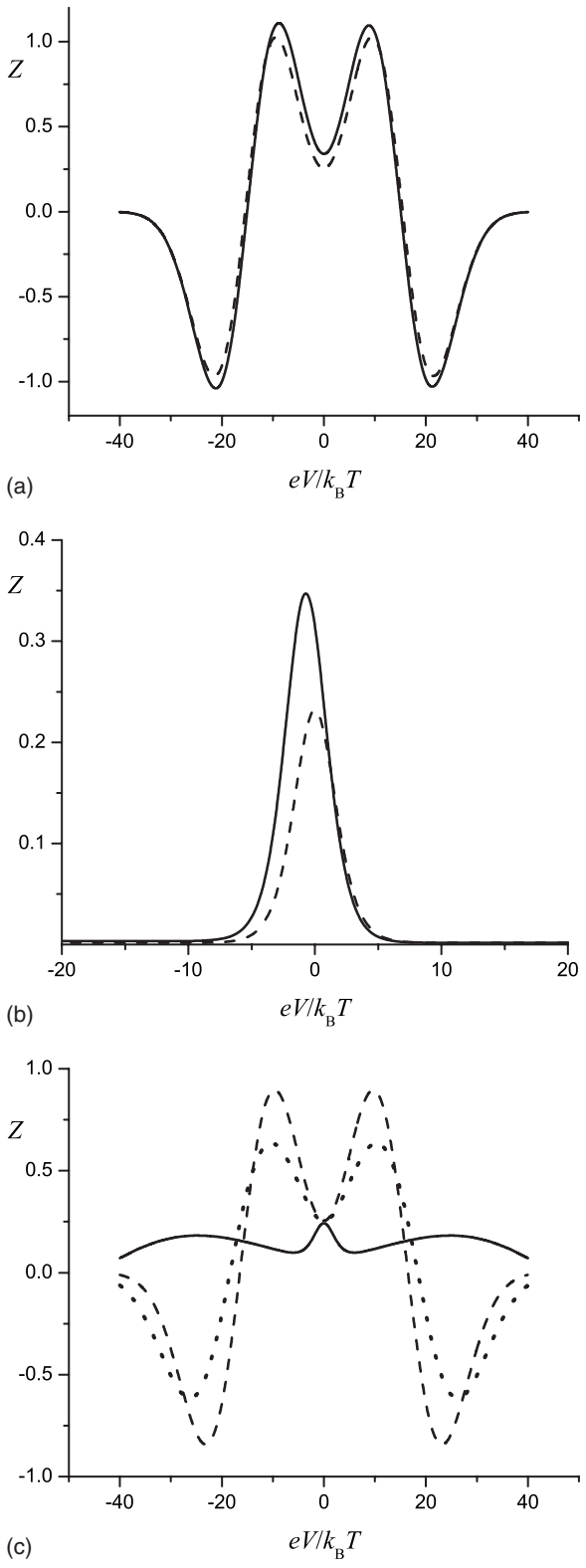

FIG. 10. Effect of Debye screening on the dependence of the differential conductance on the bias voltage for $\eta=\delta=0$, $\lambda=5k_BT$, $\lambda_{12}=2\lambda$, $z_1/L=1-z_2/L=0.15$, and $k_0/k=0.01$. (a) $L_D/L=3$, solid line: $U_{12}\to\infty$; dashed line: $U_{12}=0$; (b) $L_D/L=0.03$, solid line: $U_{12}\to\infty$; dashed line: $U_{12}=0$; and (c) $U_{12}=0$, solid line: $L_D/L=0.1$, dashed line: $L_D/L=0.5$, and dotted line: $L_D/L=0.3$. Differential conductance is normalized to $ek_0\exp(-\lambda_{12}/4k_BT)/k_BT$.

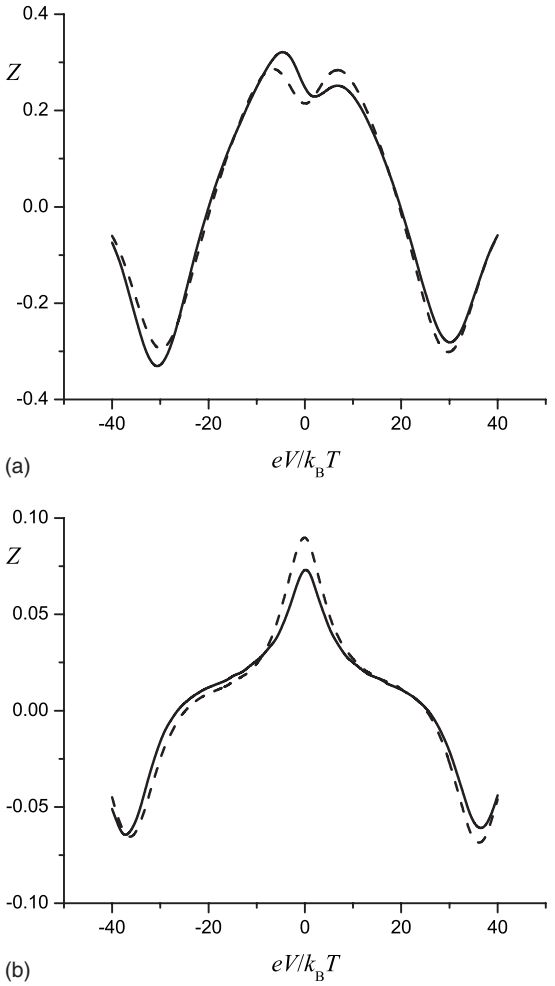

FIG. 11. Effect of k_0/k on the dependence of the differential conductance on the bias voltage for $\eta=\delta=0$, $\lambda=5k_BT$, $\lambda_{12}=2\lambda$, $z_1/L=1-z_2/L=0.15$, and $L_D/L=0.3$. Solid line: $U_{12}\to\infty$; dashed line: $U_{12}=0$. (a) $k_0/k=1$; (b) $k_0/k=10$. Differential conductance is normalized to $ek_0\exp(-\lambda_{12}/4k_BT)/k_BT$.

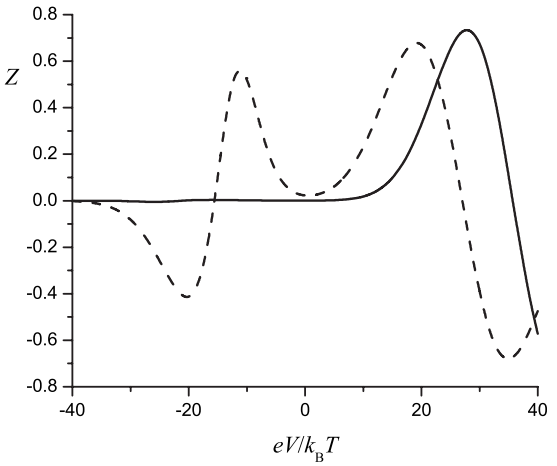

FIG. 12. Rectification of the tunnel current in the case when $\delta=-2\lambda$, $\eta=0$, $\lambda=5k_BT$, $\lambda_{12}=2\lambda$, $z_1/L=1-z_2/L=0.15$, $L_D/L=0.3$, and $k_0/k=0.01$. Solid line: $\delta=-10k_BT$; dashed line: $\delta=-5k_BT$. Differential conductance is normalized to $ek_0\exp(-\lambda_{12}/4k_BT)k_BT$.

affects also the form of the $Z(V)$ curves. When L_D/L tends to zero, γ_2, γ_1, and the difference $\gamma_2-\gamma_1$ tend to zero too so that the points of the maxima $|V_{*\pm}|$ as well as their widths tend to infinity. In this case, at $\delta=0$, the positions of the electron energy levels of quantum dots are independent of V and coincide so that $E_1(1,0)-E_2(0,1)=0$. As a result, the absolute values of the tunnel current are independent of V for $|V|>2k_BT$ [see, e.g., Eq. (12)]. Within the interval $-2k_BT<V<2k_BT$ the tunnel current increases rapidly from negative to positive values which results in the sharp U_{12}-dependent peaks in the $Z(V)$ curves [Fig. 10(b)]. Figure 10(c) shows that, with the increase in L_D/L, the transition from the $Z(V)$ curves having two maxima to $Z(V)$ curves having only single maximum at $V=0$ is continuous and includes the curves having three maxima. It can be shown that a maximum at $V=0$ appears when $6\gamma_2-3\gamma_2^2-3\gamma_1-2<0$ or when $L_D/L<0.174$.

We consider so far only the case of small values of k_0/k. A value of k_0/k also strongly affects a form of a $Z(V)$ curve. The normalized differential conductance which is proportional to Z/k_0 behaves approximately as $P(1,0)/k_0$ or $P(0,1)/k_0$ at the points of maxima of Z and, therefore, decreases with the increase in k_0/k. A value of Z/k_0 at $V=0$ decreases more slowly with the increase in k_0/k [see Eq. (A14)]. As a result, with the increase in k_0/k, values of Z/k_0 at $V\approx 0$ and $V_{\max,\pm}$ approaches each other [see Fig. 11(a)] and, finally, for rather large values of k_0/k, merge into a single maximum at $V=0$ [see Fig. 11(b)].

Concluding this section, we address briefly the problem of rectification of the tunnel current by the two quantum dot system discussed first in Ref. 22. The simplest way to treat this problem can be based on Eq. (16). As follows from Eq. (16), a value of V_{*-} equal zero at $\delta=-2\lambda$. Since the tunnel current and, hence, Z are proportional to $\exp(-\delta^2/8\lambda k_BT)\exp(-|\delta|/2k_BT)$ at $V=\eta=0$ [see Eq. (12)], the tunnel current in the region $V<0$ is almost zero for $\delta=-2\lambda$. Figure 12 illustrates this conclusion and shows that $Z(V)\approx 0$ for $V\leq 0$ in the case when $\delta=-2\lambda$. For $\delta=-\lambda$ a complete rectification is absent. It should be noted that, in contrast to Ref. 22 where a molecular rectifier in vacuum was considered, the use of the double quantum dot system in combination with the electrolyte solution permits to tune a rectification by variations in the gate voltage, the interdot Coulomb repulsion energy, the energy of the polaron shift, and the intensity of the Debye screening. A detail analysis of the problem of the rectification by the double quantum dot system from this point of view will be given elsewhere.

V. CONCLUSION

In this paper the effect of the interdot Coulomb repulsion on the tunnel current/gate voltage dependence for the double quantum dot system in the serial configuration in the totally weak tunneling limit with due account of the strong electron-phonon interaction and Debye screening effect is studied. It is shown that in the small k_0/k limit and at rather large values of the interdot Coulomb repulsion the tunnel current/gate voltage curve has a large width at half maximum which has the order of $-k_BT\ln(k_0/k)$. The double quantum dot system in this regime can be used as an amplifier where the ampli-

fication takes place in the wide range of values of the gate voltage. A consequence of the strong Coulomb blockade in the small k_0/k and large U_{12} limits is also the dependence of the position of the maximum of the current/gate voltage curve and its width on the energy λ of the polaron shift. Since the critical values U_{12*} of U_{12} have the order of the width $W[\approx -k_BT\ln(k_0/k)]$ at small ratio k_0/k, the Coulomb blockade peaks appear at rather large values of the gate voltage η in this case. At $k_0/k \geq 1$ the effect of the interdot Coulomb repulsion manifests itself in the narrow-width Coulomb blockade peaks in the tunnel current/gate voltage curves. The shape of these curves is similar to that obtained for the one-level quantum dot[16] but the peaks have different physical interpretation. Another interesting feature of the electron correlation effects arising due to the interdot Coulomb repulsion is the dependence of the positions of the maxima of the current/gate voltage dependence and their widths on the sign of the difference of the electron energy levels of the quantum dots.

The effect of the interdot Coulomb repulsion on the differential conductance/bias voltage dependence is also studied. This effect consists mainly in the violation of the identity $Z(V,\eta,\delta)=Z(-V,-\eta,-\delta)$ which takes place at $U_{12}=0$ and in the strong dependence of the maximum and minimum values of the differential conductance in the region $V<0$ on U_{12}. In addition to that, the form of the $Z(V)$ curve depends on the gate voltage, the difference of the electron energy levels of the quantum dots, the Debye screening length, and a value of k_0/k. As a result, the form of the $Z(V)$ curve can be very different in different regions of the parameter space so that it is possible to make a conclusion about the physical parameters of the system basing on the characteristic forms of these curves. The existence of the regions of the negative differential conductance is demonstrated and the dependence of their positions on the parameters of the system is studied. The problem of rectification of the tunnel current by the two quantum dot system is briefly addressed.

ACKNOWLEDGMENTS

The author is grateful to A. M. Kuznetsov for helpful discussions. This work was partially supported by the Russian Foundation for Basic Research under Grant No. 09-03-00317a.

APPENDIX

Here we present the expressions for the steady-state probabilities $P(n_1,n_2)$ and study the dependence of $P(n_1,n_2)$ and the tunnel current on the parameters of the system for different limiting cases for two opposite values of U_{12}: $U_{12}=0$ and $U_{12}\to\infty$. The steady-state solutions of Eqs. (1)–(3) have the form

$$P(0,0)=\frac{k_{1L}(1,0)P(1,0)+k_{2R}(0,1)P(0,1)}{k_{L1}(0,0)+k_{R2}(0,0)},$$

$$P(1,1)=\frac{k_{L1}(0,1)P(0,1)+k_{R2}(1,0)P(1,0)}{k_{1L}(1,1)+k_{2R}(1,1)}, \quad \text{(A1)}$$

$$P(1,0)=\frac{2D_{01}}{D_{01}G_{10}+D_{10}G_{01}}, \quad P(1,0)=\frac{2D_{10}}{D_{01}G_{10}+D_{10}G_{01}}, \quad \text{(A2)}$$

where

$$D_{10}=k_{12}(1,0)+\frac{k_{R2}(0,0)k_{1L}(1,0)}{k_{L1}(0,0)+k_{R2}(0,0)}+\frac{2k_{1L}(1,1)k_{R2}(1,0)}{k_{1L}(1,1)+k_{2R}(1,1)}, \quad \text{(A3)}$$

$$D_{01}=k_{21}(0,1)+\frac{k_{L1}(0,0)k_{2R}(0,1)}{k_{L1}(0,0)+k_{R2}(0,0)}+\frac{2k_{2R}(1,1)k_{L1}(0,1)}{k_{1L}(1,1)+k_{2R}(1,1)}, \quad \text{(A4)}$$

$$G_{10}=2+\frac{k_{1L}(1,0)}{k_{L1}(0,0)+k_{R2}(0,0)}+\frac{4k_{R2}(1,0)}{k_{1L}(1,1)+k_{2R}(1,1)}, \quad \text{(A5)}$$

$$G_{01}=2+\frac{k_{2R}(0,1)}{k_{L1}(0,0)+k_{R2}(0,0)}+\frac{4k_{L1}(0,1)}{k_{1L}(1,1)+k_{2R}(1,1)}. \quad \text{(A6)}$$

1. The case when $U_{12}=0$

In this case $k_{L1}(0,1)=k_{L1}(0,0)$, $k_{1L}(1,1)=k_{1L}(1,0)$, $k_{R2}(1,0)=k_{R2}(0,0)$, and $k_{2R}(1,1)=k_{2R}(0,1)$. We start from the limit $k_0/k\to 0$. Using Eqs. (A1)–(A6) one obtains that

$$P(0,0)=\frac{k_{1L}(1,0)k_{2R}(0,1)}{Z}, \quad P(1,1)=\frac{4k_{L1}(0,0)k_{R2}(0,0)}{Z}, \quad \text{(A7)}$$

$$P(1,0)=\frac{2k_{L1}(0,0)k_{2R}(0,1)}{Z}, \quad P(0,1)=\frac{2k_{R2}(0,0)k_{1L}(1,0)}{Z}, \quad \text{(A8)}$$

where

$$Z=k_{1L}(1,0)k_{2R}(0,1)+2[k_{L1}(0,0)k_{2R}(0,1)+k_{R2}(0,0)k_{1L}(1,0)]+4k_{L1}(0,0)k_{R2}(0,0). \quad \text{(A9)}$$

Then it follows from Eqs. (8) and (A8) that the tunnel current with the accuracy up to the first order in k_0/k is given by the expression

$$j=\frac{2e[k_{L1}(0,0)k_{12}(1,0)k_{2R}(0,1)-k_{R2}(0,0)k_{21}(0,1)k_{1L}(1,0)]}{Z}. \quad \text{(A10)}$$

Finally, using the detailed balance principle [Eq. (5)], we obtain Eqs. (10), (12), and (13) which are valid for arbitrary values of V, η, λ, and Δ.

For arbitrary values of k_0/k the dependence of the tunnel current on the parameters of the system can be studied analytically only in the large λ limit when, e.g., $k_{L1}(0,0)\approx 0.5\pi k\exp(-\lambda/4k_BT)\exp[\Delta F_{1L}(0,0)/2k_BT]$. It can be shown that in this limit

$$j = \frac{2^{1/2} e k_0 \exp\left(-\frac{\lambda_{12}}{4k_BT}\right) \mathrm{ch}\left(\frac{2e\xi\eta - e\xi V + \delta}{4k_BT}\right) \mathrm{sh}\left(\frac{eV}{2k_BT}\right)}{aF + 2^{3/2} \mathrm{ch}\left(\frac{2e\xi\eta - e\xi V + \delta}{4k_BT}\right) \mathrm{ch}\left(\frac{e\xi\eta + e\gamma_1 V}{2k_BT}\right) \mathrm{ch}\left(\frac{e\xi\eta + e(\gamma_2 - 1)\xi V + \delta}{2k_BT}\right)}, \tag{A11}$$

where

$$a = \frac{2k_0 \exp(-\lambda_{12}/4k_BT)}{\pi k \exp(-\lambda/4k_BT)} \tag{A12}$$

and

$$F = \mathrm{ch}\left(\frac{eV - \Delta}{4k_BT}\right) \mathrm{ch}\left(\frac{\Delta}{2k_BT}\right) + \mathrm{ch}\left(\frac{eV + \Delta}{4k_BT}\right) \mathrm{ch}\left(\frac{2e\xi\eta - e\xi V + \delta}{2k_BT}\right). \tag{A13}$$

At $a=0$ Eq. (A11) yields the large λ limit of Eq. (12). The tunnel current given by Eq. (A11) has the symmetry property $j(V,\eta,\delta) = -j(-V,-\eta,-\delta)$ for all values of k_0/k in the large λ limit. It follows from Eq. (A11) that, as in the $k_0/k \to 0$ limit, the tunnel current takes its maximum values at $\eta_{\max} = V/2 - \delta/2e\xi$ for all values of k_0/k. However, the width W at half maximum of the $j(\eta)$ curve depends on the ratio k_0/k. For example, a value of $\mathrm{ch}(e\xi W/4k_BT)$ equals $[-a + (a^2 + 128^{1/2}a + 16)^{1/2}]/8^{1/2}$ for $|eV|, |\Delta| \ll k_BT$ and increases monotonously from $2^{1/2}$ for $a=0$ to 2 for $a \to \infty$. As a result, the width $e\xi W$ increases monotonously from $4k_BT \ln[1+2^{1/2}]$ to $4k_BT \ln[2+3^{1/2}]$ when k_0/k increases from 0 to infinity.

The expression for the differential conductance $Z(V) = dj/d(eV)$ can be readily obtained from Eq. (A11). In particular, for $V=\Delta=0$, one obtains that

$$Z(0) = \frac{1}{4k_BT} \frac{2^{1/2} e k_0 \exp(-\lambda_{12}/4k_BT)}{a \mathrm{ch}(e\xi\eta/2k_BT) + 2^{1/2} \mathrm{ch}^2(e\xi\eta/2k_BT)}. \tag{A14}$$

The differential conductance given by Eq. (A14) is independent of L_D for $\eta=0$ and decreases with increase in the absolute value of η. The ratio Z/k_0 decreases with the increase in k_0.

We also discuss briefly the limit $k_0/k \to \infty$. From Eq. (A11) one obtains that

$$j = 2^{1/2} \frac{\pi}{2} ek \exp\left(-\frac{\lambda}{4k_BT}\right) \times \mathrm{ch}\left(\frac{2e\xi\eta - e\xi V + \delta}{4k_BT}\right) \mathrm{sh}\left(\frac{eV}{2k_BT}\right) \Big/ F \tag{A15}$$

in this limit. Using Eqs. (A13) and (A15) the expression for the width W at half maximum of the $j(\eta)$ curve can be obtained. It follows from this expression that $e\xi W \approx 4k_BT \ln[2+3^{1/2}]$ in the case when $|eV|, |\Delta| \ll k_BT$ or $|eV| \gg |\Delta|, k_BT$ and $e\xi W \approx 2|\Delta|$ in the case when $|\Delta| \gg |eV|, k_BT$. The last value of $e\xi W$ is twice larger then that in the limit $k_0/k \to 0$ since the larger values of k_0/k make available large values of the tunnel current in the larger interval of $\xi\eta$.

2. The case when $U_{12} \to \infty$

The last terms on the rhs of Eqs. (A3)–(A6) should be omitted in this case. Then the expression for the tunnel current has the form

$$j = 2e[k_{L1}(0,0)k_{12}(1,0)k_{2R}(0,1) - k_{R2}(0,0)k_{21}(0,1)k_{1L}(1,0)]/D, \tag{A16}$$

where

$$D = 2[k_{21}(0,1) + k_{12}(1,0)][k_{L1}(0,0) + k_{R2}(0,0)] + k_{21}(0,1)k_{1L}(1,0) + k_{12}(1,0)k_{2R}(0,1) + 2[k_{L1}(0,0)k_{2R}(0,1) + k_{1L}(1,0)k_{R2}(0,0)] + k_{1L}(1,0)k_{2R}(0,1).$$

As in the case when $U_{12}=0$, we start from the limit $k_0/k \to 0$. In this limit

$$P(0,0) = \frac{k_{1L}(1,0)k_{2R}(0,1)}{Z_\infty}, \quad P(1,0) = \frac{2k_{L1}(0,0)k_{2R}(0,1)}{Z_\infty}, \quad P(0,1) = \frac{2k_{1L}(1,0)k_{R2}(0,0)}{Z_\infty}, \tag{A17}$$

where

$$Z_\infty = k_{1L}(1,0)k_{2R}(0,1) + 2[k_{L1}(0,0)k_{2R}(0,1) + k_{1L}(1,0)k_{R2}(0,0)]. \tag{A18}$$

Then, using the detailed balance principle [Eq. (5)] and Eqs. (A16)–(A18), we obtain Eqs. (11), (12), and (15) which are valid for arbitrary values of V, η, λ, and Δ. As was discussed in Sec. III of the paper, the tunnel current given by Eq. (15) increases monotonously with the increase in η so that the current is not maximum at the finite value of $\eta = \eta_{\max}$. This maximum appears when the contribution of the term on the order of k_0/k in the denominator of the expression for the current is taken into account.

It follows from Eq. (A16) that in the large λ limit

$$j = \frac{2ek_0 \exp\left(-\frac{\lambda_{12}}{4k_BT}\right)\mathrm{sh}\left(\frac{eV}{2k_BT}\right)}{2^{1/2}aF_\infty + 2\mathrm{ch}\left(\frac{eV-\Delta}{2k_BT}\right) + \exp\left(\frac{-2e\xi\eta + e\xi V - \delta}{2k_BT}\right)}, \tag{A19}$$

where

$$F_\infty = 2\exp\left(\frac{2e\xi\eta - e\xi V + \delta}{4k_BT}\right)\mathrm{ch}\left(\frac{eV-\Delta}{4k_BT}\right)\mathrm{ch}\left(\frac{\Delta}{2k_BT}\right) + \exp\left(\frac{-2e\xi\eta + e\xi V - \delta}{4k_BT}\right)\mathrm{ch}\left(\frac{eV+\Delta}{4k_BT}\right) \tag{A20}$$

and a is given by Eq. (A12). At $a=0$ Eq. (A19) yields the large λ limit of Eq. (15). However, the tunnel current in the infinite U_{12} limit does not have the symmetry property $j(V,\eta,\delta)$ $=-j(-V,-\eta,-\delta)$ which takes place at $U_{12}=0$ by the reason discussed in Sec. IV. Using Eqs. (A19) and (A20) it can be shown that in the small k_0/k limit

$$e\xi\eta_{\max,\infty} \approx (\xi eV - \delta)/2 + \lambda/6 - 2k_BT\ln(k_0/k)/3 - 2k_BTf/3 \tag{A21}$$

with the accuracy up to the terms of the order of $\ln(k_0/k)$, where

$$f = \ln\left[\mathrm{ch}\left(\frac{eV-\Delta}{4k_BT}\right)\mathrm{ch}\left(\frac{\Delta}{2k_BT}\right)\right] + \ln\left(\frac{4\sqrt{2}}{\pi}\right). \tag{A22}$$

Using Eq. (A16) it can be shown that, for all values of λ in the small k_0/k limit,

$$j(\eta_{\max,\infty}) = ek_0 \exp\left(-\frac{\Delta^2}{4\lambda_{12}k_BT}\right) \times \exp\left(-\frac{\lambda_{12}}{4k_BT}\right)\mathrm{sh}\left(\frac{eV}{2k_BT}\right) \Big/ \mathrm{ch}\left(\frac{eV-\Delta}{2k_BT}\right). \tag{A23}$$

In contrast to the case $U_{12}=0$, the rhs of the expression for $e\xi\eta_{\max,\infty}$ includes three additional terms which take into account electron correlation effects and depend on the polaron shift, V, δ, and $\ln(k_0/k)$. When $|eV| \gg |\delta|$, k_BT and $|\Delta| \ll k_BT$, one obtains that

$$e\xi\eta_{\max,\infty} \approx (1-\gamma_2-2\gamma_1)eV/3 + \lambda/6 - 2k_BT\ln(k_0/k)/3. \tag{A24}$$

Therefore, in the limit $L_D/L \to 0$, $e\xi\eta_{\max}$ varies as $eV/3$ with the increase in V but not as $eV/2$. The most interesting is the dependence of $e\xi\eta_{\max,\infty}$ on δ in the case when $|\delta| \gg |eV|$, k_BT. It follows from Eqs. (A21) and (A22) that

$$e\xi\eta_{\max,\infty} \approx -\delta/2 - |\delta|/2 + \lambda/6 - 2k_BT\ln(k_0/k)/3 \tag{A25}$$

in this case. Equation (A25) shows that $e\xi\eta_{\max,\infty}$ varies as $-\delta$ for $\delta>0$ and is independent of δ for $\delta<0$. We also present the expressions for $e\xi\eta_{\max,\infty}$ for two practically important particular cases in which $|eV|$ and $|\Delta|$ have the same order. In the first case $\Delta<0$, $V>0$, $|eV-\Delta| \gg k_BT$, and $|\Delta| \gg k_BT$. Then

$$e\xi\eta_{\max,\infty} \approx (1-3\gamma_1)eV/3 + \lambda/6 - 2k_BT\ln(k_0/k)/3. \tag{A26}$$

In the second case $\delta>0$, $V>0$, $|eV-\Delta| \ll k_BT$, and $\Delta \gg k_BT$. Then

$$e\xi\eta_{\max,\infty} \approx (3-5\gamma_2-\gamma_1)eV/6 - 5\delta/6 + \lambda/6 - 2k_BT\ln(k_0/k)/3. \tag{A27}$$

It follows from Eqs. (A19) and (A20) that the width W at half maximum of the $j(\eta)$ curve in the large λ and small k_0/k limits calculated with the accuracy up to the terms of the order of $\ln(k_0/k)$ is given by the expression

$$e\xi W \approx \lambda/2 - 2k_BT\ln(k_0/k) + k_BT\ln\left[\frac{2\mathrm{ch}^3\left(\frac{eV-\Delta}{2k_BT}\right)}{\mathrm{ch}^2\left(\frac{\Delta}{2k_BT}\right)\mathrm{ch}^2\left(\frac{eV-\Delta}{4k_BT}\right)}\right] + 2k_BT\ln(\pi/2). \tag{A28}$$

When $|eV| \gg |\delta|$, k_BT and $|\Delta| \ll k_BT$, we have that

$$e\xi W \approx (1-\gamma_2+\gamma_1)eV + \lambda/2 - 2k_BT\ln(k_0/k). \tag{A29}$$

When $|\delta| \gg |eV|$, k_BT, one obtains that

$$e\xi W \approx |\delta|/4 + \lambda/2 - 2k_BT\ln(k_0/k). \tag{A30}$$

Figures presented in Sec. III show that the main parts of the $j(\eta)$ curves lie in the region, where $|e\xi\eta| < \lambda$ in the case when $\delta>0$. The points $e\xi\eta_{\max,\infty}$ lie also in this region in the case when $\delta \le 0$. However, when $\delta \le 0$, the points $e\xi(\eta_{\max,\infty}+W/2)$ lie in the region, where $|e\xi\eta| > \lambda$. Therefore, in order to calculate the width of the $j(\eta)$ curves in the case when $\delta \le 0$, the expression for the tunnel current in the large $e\xi\eta$ region ($e\xi\eta \gg \lambda$) should be obtained. It can be shown[19] that in the large $e\xi\eta$ limit $k_{L1}(0,0)=k_{R2}(0,0)$ $=k(\pi\lambda/k_BT)^{1/2}$. The rate constants $k_{1L}(1,0)$ and $k_{2R}(0,1)$ are very small in this limit. The expressions for these constants can be obtained using the detailed balance principle [Eq. (5)]. Then the expression for the tunnel current has the same form as Eq. (A19)

$$j = \frac{2ek_0 \exp\left(-\frac{\lambda_{12}}{4k_BT}\right)\mathrm{sh}\left(\frac{eV}{2k_BT}\right)}{a'F'_\infty + 2\mathrm{ch}\left(\frac{eV-\Delta}{2k_BT}\right) + \exp\left(\frac{-2e\xi\eta + e\xi V - \delta}{2k_BT}\right)}, \tag{A31}$$

where a and F_∞ should be replaced by a' and F'_∞. Here a' $=k_0\exp(-\lambda_{12}/4k_BT)/[k(\pi\lambda/k_BT)^{1/2}]$ and

$$F'_\infty = 2\exp\left(\frac{2e\xi\eta - e\xi V + \delta}{2k_BT}\right)\mathrm{ch}\left(\frac{\Delta}{2k_BT}\right) + \mathrm{ch}\left(\frac{eV}{2k_BT}\right). \tag{A32}$$

At $a'=0$ Eq. (A31) also yields the large λ limit of Eq. (16).

Then it follows from Eqs. (A31) and (A32) that the width W for $\delta \leq 0$ in the large $e\xi\eta$ and small k_0/k limits calculated with the accuracy up to the terms on the order of $\ln(k_0/k)$ is given by the expression

$$e\xi W \approx \lambda/2 - k_B T \ln(k_0/k) + k_B T \ln\left[\frac{2\mathrm{ch}^2\left(\frac{eV-\Delta}{2k_B T}\right)}{\mathrm{ch}\left(\frac{\Delta}{2k_B T}\right)}\right] + k_B T \ln(\pi\lambda/k_B T)/2. \quad \text{(A33)}$$

The rhs of Eq. (A33) differs from that of Eq. (A28) by the factor at $\ln(k_0/k)$ and the terms which include logarithmic functions. As a result, one obtains that, in the limit $|\delta| \gg |eV|$, $k_B T$, and $\delta \leq 0$,

$$e\xi W \approx |\delta|/2 + \lambda/2 - k_B T \ln(k_0/k). \quad \text{(A34)}$$

It follows from Eqs. (A30) obtained for $\delta > 0$ and Eq. (A34) obtained for $\delta \leq 0$ that the width depends on the sign of δ.

Finally we address the limit $k_0/k \to \infty$. When U_{12} is finite but large enough, the overlap between the first and the second peaks of the $j(\eta)$ curve is almost absent in this limit. Then it follows from Eqs. (A12) and (A19) that in the large λ limit the tunnel current j_1 in the neighborhood of the first peak is given approximately by the expression

$$j_1 = 2^{1/2}\frac{\pi}{2} ek \exp\left(-\frac{\lambda}{4k_B T}\right)\mathrm{sh}\left(\frac{eV}{2k_B T}\right) \Big/ F_\infty \quad \text{(A35)}$$

and coincides with the total tunnel current in the limit $U_{12} \to \infty$. When $\delta = 0$ and $\gamma_1 = \gamma_2 = \gamma$ (the positions of both levels are the same), Eq. (A35) coincides formally with the expression for the tunnel current in the spinless model in the case of the single-center bridged contact [see Eq. (21) of Ref. 17, where $\Delta_{el} = \Delta_{tip} = k\hbar(\pi\lambda/k_B T)^{1/2}/2$] having single nondegenerate electron energy level where, however, the parameter $e\xi\eta$ is shifted by $-k_B T \ln(2)$

$$j_1 = \frac{\frac{\pi}{2} ek \exp\left(-\frac{\lambda}{4k_B T}\right)\mathrm{sh}\left(\frac{eV}{4k_B T}\right)}{\mathrm{ch}\left[\frac{e\xi\eta - k_B T \ln(2) - e(0.5-\gamma)V}{2k_B T}\right]}. \quad \text{(A36)}$$

In the model under consideration when the spin degeneracy is taken into account, Eq. (A35) describes the tunnel current in the case of the single-center bridged contact having doubly degenerate electron energy level ($\varepsilon_1 = \varepsilon_2$), which can be occupied by single electron due to $U_1 = U_2 = U_{12} = \infty$). The shift $-k_B T \ln(2)$ of $\xi\eta$ is due to the entropy contribution to the free energies ΔF.

It can be shown using Eq. (A35) that the tunnel current j_1 takes its maximum value at

$$e\xi\eta_{\max,1} = (\xi eV - \delta)/2 - k_B T \ln(2) + k_B T \ln\left\{\frac{\mathrm{ch}[(eV+\Delta)/4_B T]}{\mathrm{ch}[(eV-\Delta)/4k_B T]\mathrm{ch}(\Delta/2k_B T)}\right\} \quad \text{(A37)}$$

so that

$$j_1(\eta_{\max,1}) = \frac{\frac{\pi}{2} ek \exp\left(-\frac{\lambda}{4k_B T}\right)\mathrm{sh}\left(\frac{eV}{2k_B T}\right)}{2\left[\mathrm{ch}\left(\frac{eV-\Delta}{4k_B T}\right)\mathrm{ch}\left(\frac{\Delta}{2k_B T}\right)\mathrm{ch}\left(\frac{eV+\Delta}{4k_B T}\right)\right]^{1/2}}. \quad \text{(A38)}$$

As $e\xi\eta_{\max,\infty}$ in the limit $k_0/k \to 0$, $e\xi\eta_{\max,1}$ varies as $-\delta$ for $\delta > 0$ and is independent of δ for $\delta < 0$ in the case when $|\delta| \gg |eV|$, $k_B T$

$$e\xi\eta_{\max,1} \approx c_1 eV - \delta/2 - |\delta|/2, \quad \text{(A39)}$$

where $c_1 = 1 - \gamma_2$ for $\delta > 0$ and $c_1 = -\gamma_1$ for $\delta < 0$. It can also be shown that $e\xi\eta_{\max,1}$ is given by Eq. (13) for $|eV| \gg |\delta|$, $k_B T$ and is smaller than the rhs of Eq. (13) by $k_B T \ln(2)$ in the case when $|eV|$, $|\delta| \ll k_B T$.

It follows from Eqs. (A35) and (A37) that, in contrast to all cases considered above, the width $e\xi W$ in the limit $k_0/k \to \infty$ equals $4k_B T \ln(2+3^{1/2})$ and, therefore, is independent of V, λ, L_D, and δ.

The approximate expression j_2 for the tunnel current near the second peak of the $j(\eta)$ curve can be obtained if one neglects the second terms on the rhs of Eqs. (A3)–(A6). Then this expression has a form of Eq. (A35) where the denominator $F_{\infty 2}$ is slightly different from F_∞. Namely, the energy $e\xi\eta$ is replaced by $e\xi\eta' = e\xi\eta - U_{12}$ and the exponential factors on the rhs of Eq. (A20) are interchanged

$$F_{\infty 2} = 2\exp\left(\frac{-2e\xi\eta' + e\xi V - \delta}{4k_B T}\right)\mathrm{ch}\left(\frac{eV-\Delta}{4k_B T}\right)\mathrm{ch}\left(\frac{\Delta}{2k_B T}\right) + \exp\left(\frac{2e\xi\eta' - e\xi V + \delta}{4k_B T}\right)\mathrm{ch}\left(\frac{eV+\Delta}{4k_B T}\right). \quad \text{(A40)}$$

As a result, the expression for the position $\eta_{\max,2}$ of the Coulomb blockade peak has a form of Eq. (A37) where, however, U_{12} is added to the rhs and the last term enters the rhs with an opposite sign

$$e\xi\eta_{\max,2} = U_{12} + (\xi eV - \delta)/2 + k_B T \ln(2) - k_B T \ln\left\{\frac{\mathrm{ch}[(eV+\Delta)/4_B T]}{\mathrm{ch}[(eV-\Delta)/4_B T]\mathrm{ch}(\Delta/2k_B T)}\right\}. \quad \text{(A41)}$$

The height $j(\eta_{\max,2})$ of the Coulomb blockade peak and its width coincide with those for the first peak. It can be shown that $e\xi\eta_{\max,2} = U_{12} + e\xi\eta_{\max}$ for $|eV| \gg |\delta|$, $k_B T$, where $\eta_{\max}$ is given by Eq. (13). However, in contrast to the behavior of the position of the maximum of the first peak [Eq. (A39)], $\xi\eta_{\max,2}$ is independent of δ for $\delta > 0$ and varies as $|\delta|$ for $\delta < 0$ in the case when $|\delta| \gg |eV|$, $k_B T$

$$e\xi\eta_{\max,2} \approx c_2 eV - \delta/2 + |\delta|/2, \quad \text{(A42)}$$

where $c_2 = -\gamma_1$ for $\delta > 0$ and $c_2 = 1 - \gamma_2$ for $\delta < 0$.

It is worth noting that if we consider the sum $j(\eta_{\max,1}) + j(\eta_{\max,2})$ and formally take the limit $U_{12} \to 0$, we would obtain a function of η which has a maximum at the point $\eta_{\max}$ given by Eq. (13). The sum $\eta_{\max,1} + \eta_{\max,2}$ equals $2\eta_{\max}$ in this case.

[1] M. Elbing, R. Ochs, M. Koentopp, M. Fischer, C. v. Hanisch, F. Weigend, F. Evers, H. B. Weber, and M. Mayor, Proc. Natl. Acad. Sci. U.S.A. **102**, 8815 (2005).
[2] C. W. J. Beenakker, Phys. Rev. B **44**, 1646 (1991).
[3] D. V. Averin, A. N. Korotkov, and K. K. Likharev, Phys. Rev. B **44**, 6199 (1991).
[4] G. Klimeck, G. Chen, and S. Datta, Phys. Rev. B **50**, 2316 (1994).
[5] G. Chen, G. Klimeck, S. Datta, G. Chen, and W. A. Goddard, Phys. Rev. B **50**, 8035 (1994).
[6] C. Niu, L. J. Liu, and T. H. Lin, Phys. Rev. B **51**, 5130 (1995).
[7] P. Pals and A. MacKinnon, J. Phys.: Condens. Matter **8**, 5401 (1996).
[8] S. Lamba and S. K. Joshi, Phys. Rev. B **62**, 1580 (2000).
[9] R. Aguado and D. C. Langreth, Phys. Rev. B **67**, 245307 (2003).
[10] B. R. Bulka and T. Kostyrko, Phys. Rev. B **70**, 205333 (2004).
[11] Q.-Q. Xu and S.-J. Xiong, J. Phys.: Condens. Matter **18**, 10269 (2006).
[12] B. Song, D. A. Ryndyk, and G. Guniberti, Phys. Rev. B **76**, 045408 (2007).
[13] A. Hubel, K. Held, J. Weis, and K. v. Klitzing, Phys. Rev. Lett. **101**, 186804 (2008).
[14] J. Wang, X. Lu, and C.-Q. Wu, J. Phys.: Condens. Matter **19**, 496216 (2007).
[15] A. M. Kuznetsov and I. G. Medvedev, J. Phys.: Condens. Matter **20**, 374112 (2008).
[16] A. M. Kuznetsov and I. G. Medvedev, Phys. Rev. B **78**, 153403 (2008).
[17] I. G. Medvedev, Phys. Rev. B **76**, 125312 (2007).
[18] A. Mitra, I. Aleiner, and A. J. Millis, Phys. Rev. B **69**, 245302 (2004).
[19] A. M. Kuznetsov, I. G. Medvedev, and J. Ulstup, J. Chem. Phys. **127**, 104708 (2007).
[20] C. D. Mahan, *Many Particle Physics* (Plenum, New York, 1990).
[21] L. D. Landau and E. M. Lifshits, *Quantum Mechanics: Non-relativistic Theory* (Pergamon, Oxford, 1965).
[22] A. Aviram and M. A. Ratner, Chem. Phys. Lett. **29**, 277 (1974).